NASA TECHNICAL MEMORANDUM

NASA TM X-3119

NASA TM X-3119



# EXPERIMENTAL EVALUATION OF COMPLIANT SURFACES AT LOW SPEEDS

*by Kenneth W. McAlister and Tom M. Wynn*

*Ames Research Center*

*and*

*U.S. Army Air Mobility R&D Laboratory*

*Moffett Field, Calif. 94035*

NATIONAL AERONAUTICS AND SPACE ADMINISTRATION • WASHINGTON, D. C. • OCTOBER 1974

# EXPERIMENTAL EVALUATION OF COMPLIANT SURFACES AT LOW SPEEDS

Kenneth W. McAlister and Tom M. Wynn

Ames Research Center
and
U. S. Army Air Mobility Research and Development Laboratory

## SUMMARY

An experimental study was devised to determine the profile drag on a wind tunnel model partially covered with various compliant surface materials. The model consisted of a large section of constant thickness bounded fore and aft by symmetric airfoil fairings. A flat rigid plate measuring nearly 1.5 $m^2$ (16 $ft^2$) (23 percent of model wetted area), which served as the control surface, could be exchanged for four contiguous compliant panels. Specific configurations were examined in the context of the published results of two independent investigations. The flexible media generally consisted of thin polyvinylchloride membranes stretched to various tensions over trapped fluid cavities of air, water or polyethelene oxide solution, or over dry or flooded open-celled polyurethane foams. These tests were conducted in the Ames 7- by 10-Foot Subsonic Wind Tunnel over a dynamic pressure range from 50 to 1000 pascals (Re = 1.6 to $7.4 \times 10^6$ based on model chord). On the basis of very accurate direct-force cell measurements, all configurations were found to yield profile drags equal to or slightly higher than that obtained for the conventional rigid surface case. Although the variety of compliant materials tested was limited, the results indicate that the potential for practical drag-reducing applications will be limited to either high-density or high-speed flows where more sensible pressure perturbations occur.

## INTRODUCTION

Numerous theoretical and experimental studies have been published on both laminar and turbulent boundary-layer interactions with passive compliant surfaces. A general inconclusiveness remains, however, concerning both the physical mechanisms involved and the potential for practical drag-reducing applications. Since most flows are inadvertently turbulent in practice, the recent experimental findings of Blick and his co-workers (refs. 1-3) have been particularly attractive. Their investigations culminated in a particular compliant medium that reportedly interacts with its turbulent boundary layer in air with 38 percent less viscous drag than was attained on a rigid control surface. It was hypothesized that a properly tailored compliant medium promotes a reduction in the local shear stress by absorbing energy near the interface, thereby lessening the turbulent intensity in that region. To confirm this thesis, detailed hot-wire anemometer measurements of the Reynolds stress and the individual fluctuating turbulent velocity components were recorded over both rigid and flexible surfaces. The results of Blick's tests indicated that certain compliant surfaces were indeed accompanied by substantial reductions in turbulence properties near the interface. It was therefore concluded that meaningful progress had been made in effecting lower "flat plate" viscous drag as well as in understanding the physical process by which it occurs.

Shortly thereafter, an independent effort to assess the aerodynamic benefits of a compliant medium was undertaken by Lissaman and Harris (ref. 4). Once again, great care was taken to measure the turbulence properties near the interface as well as the total shear force developed over the complete metric surface. Direct skin friction coefficients therefore could be correlated with those inferred from Reynolds stress and momentum thickness distributions. The media examined consisted of polyvinylchloride films stretched to several tensions over fluid reservoirs having different viscosities. The test program was concluded, however, after no major differences were found between the numerous flexible mediums studied and the rigid control surface. In particular, no discernible boundary-layer alterations were found to accompany any test performed, even though the surface parameters were widely varied. The success of a compliant medium in effecting a drag reduction depends on the correct matching of material properties to the particular fluid with which it interacts. Therefore, these rather discouraging results would not be especially damaging to continued pursuit were it not for the fact that one configuration studied did closely match a case reported by Blick (ref. 2) as having a significant effect.

To arbitrate this controversy, an experimental program at an independent facility was proposed wherein both Blick and Lissaman would participate through technical guidance. The surfaces to be tested would not only be similar to those previously studied by these two investigators, but, in particular, would include the most promising configuration discovered by Blick (ref. 3).

## COMPLIANT SURFACE MATERIALS

Thirteen compliant configurations were investigated. In all but two cases, the interface between the air boundary layer and the compliant substrate consisted of a thin polyvinylchloride film either 0.005 (0.002) or 0.010 (0.004) cm (in.) thick. Some of the substrate materials studied were entirely fluid, comprising trapped cavities of air, water, or a solution of water and polyethelene oxide. Other substrates were composed of 0.953 cm (0.375 in.) thick flexible polyurethane slabs, which were dry or flooded with water or a water/polyethelene oxide solution. The two special cases involved a 1.27 cm thick slab of integral-skin polyurethane foam having a corrugated surface texture oriented either parallel or perpendicular to the direction of flow. Table 1 lists the various model configurations and material specifications. Sample sections of texturized integral-skin foam and 45 PPI polyurethane foam draped with polyvinylchloride film are shown in figure 1.

In order to document more thoroughly the material properties of the most promising substrate reported by Blick, a dynamic compression and shear deflection test was devised. The necessary apparatus were designed so that measurements could be performed in accordance with applicable standards set forth by the ASTM (ref. 5). Normal stress data were obtained by compressing an unbonded foam specimen (fig. 2) to one-half its original thickness at a constant rate of 25 mm/min, and then allowing it to expand to its original thickness at the same rate. The specimen was immediately subjected to a second deformation cycle to establish the presence of hysteresis. The results shown in figure 3 indicate that even over the initial compression phase of the cycle the material does not display the normal Hookian behavior. However, by disregarding the first few percent of strain, a somewhat linear stress-strain relation develops over which an elastic modulus has been calculated. These data are primarily intended to indicate the general compressiveness of the material in several wetted states and should be viewed as qualitative. A similar procedure was developed for obtaining shear moduli of the foam in different states. For this test, the slab specimen

TABLE 1.– MODEL CONFIGURATIONS

| Model | Compliant skin thickness cm (in.) | Skin tension, N/cm (lb/in.) | Damping substrate |
|---|---|---|---|
| 1 | Rigid plate | --- | --- |
| 2 | 0.005 (0.002) PVC[a] | 0.40 (0.23) | Air |
| 3 | .005 ( .002) PVC | .82 ( .47) | Air |
| 4 | .005 ( .002) PVC | .16 ( .09) | Water |
| 5 | .005 ( .002) PVC | .40 ( .23) | Water |
| 6 | .005 ( .002) PVC | .82 ( .47) | Water |
| 7 | .010 ( .004) PVC | 1.07 ( .61) | Water |
| 8 | .005 ( .002) PVC | .26 ( .15) | Polyethylene oxide[b] |
| 9 | .005 ( .002) PVC | .26 ( .15) | Dry foam[c] |
| 10 | .005 ( .002) PVC | .26 ( .15) | Water saturated foam |
| 11 | .005 ( .002) PVC | .26 ( .15) | Polyethelene oxide saturated foam |
| 12 | Integral-skin foam,[d] grain parallel to flow | | |
| 13 | Integral-skin foam, grain perpendicular to flow | | |

[a]PVC (polyvinylchloride) film manufactured by Clopay Corporation, Cincinnati, Ohio. Clopane types used: No. 3510 (0.005 cm) and No. 3520 (0.01 cm).

[b]Polyethylene oxide type WSR-301 water-soluble resin obtained from Union Carbide Corporation, New York, N. Y. Solution used: 1.5 percent resin by weight dissolved in water (yields approximately 10,000 cP).

[c]Fully open 45 PPI (pores per inch), flexible, ester type polyurethane foam, manufactured by Scott Paper Co., Chester, Pennsylvania. Foam thickness: 0.953 cm (0.375 in.) having continuous fiber linkage. Density: 32 kg/m$^3$ (2 lb/ft$^3$).

[d]Fully open 70 PPI, flexible, ester type polyurethane foam having a texturized micropore skin on one surface. Marketed under the trade name "Coustex," by Scott Paper Co., Chester, Pennsylvania. Total thickness: 1.27 cm (0.50 in.). Maximum depth of texture: 0.15 cm (0.06 in.). Density 32 kg/m$^3$.

had to be bonded to the apparatus and care taken to use only a thin film of adhesive to prevent contamination of the flexible segments within the foam structure. The apparatus and results are shown in figures 4 and 5.

## MODEL DESCRIPTION

The complete model (fig. 6) measured 2.65 m (8.7 ft) chord, 1.88 m (6.2 ft) span, and 89 mm (3.5 in.) thick, and was fixed horizontally in the center of the Ames 7- by 10-Foot Wind Tunnel by two outboard struts. End plates extending about 14 cm (5.5 in.) above and below the model surface were attached for flow control. The NACA 66-021 airfoil section was chosen for the leading and trailing edge fairings due to its low profile drag. Narrow strips of fiberglass tape were placed near the leading edge on the upper and lower surfaces, functioning as trips to ensure flow repeatability during the initial boundary-layer development.

The model was composed of three major spanwise sections. The two outboard sections were fixed to the tunnel floor by rigid struts as well as interconnected fore and aft by tubular spars

passing through the center section. The center section in turn was entirely supported by four flexures designed to permit a collinear deflection relative to the fixed outboard sections when the model was acted upon by a streamwise force. Two Bytrex load cells, each having a 111 (25 lbf) capacity, were mounted so as to resist this rearward motion and thereby provide a direct measurement of the profile drag on the center section.

Aside from the leading and trailing edge fairings, the model was of constant thickness. The innermost portion of the upper surface on the center section was a rigid reference plate, which could be exchanged for four contiguous panels containing any given compliant medium. Each panel measured about 30 cm (12 in.) wide, 122 cm (48 in.) long, and 0.95 cm (0.375 in.) deep. The composite area measured nearly 1.5 $m^2$ (16 $ft^2$) and accounted for 23 percent of the wetted area on which the profile drag developed. To ensure relatively constant pressure in this region, the leading and trailing fairings were made more distant by an approach and retreat section over which further flow adjustments to the thickness change could occur. Figure 7 shows the pressure distribution as measured by Statham 2.5 psid transducers. A portion of the lower surface is seen to depart from the desired distribution due to the presence of the supporting struts.

## TEST PROCEDURE

Since the state of stress of PVC film is both temperature and time dependent, care was taken to maintain the air in the compliant-panel preparation area and in the wind tunnel circuit equal to ambient conditions, and to expedite every setup activity whenever practical.

Preparation of a compliant panel began with the stretching of a sheet of PVC at the required tension (fig. 8). The four clamped edges were drawn over bearing-supported rollers with appropriate weights suspended from each clamp to yield equal tensions in both directions. The thickness of the rubber pad lying beneath the stretched PVC was slightly less than the diameter of the rollers to prevent the PVC from sagging. An additional sheet of PVC was made ready on a second stretching table so that a complete set of compliant panels could be prepared simultaneously. Both sheets of PVC were then allowed to age under tension for about one hour. If required, a continuous slab of 45 PPI foam could be cut and secured within each panel using several strips of double-sided tape. (The foam had already been precut to the proper thickness by the supplier to match the depth of the panels.) After aging of the PVC, a fillet of Devcon "Zip Grip 10" adhesive was applied to the rim of each panel. The panels were then quickly inverted and pressed against the PVC and allowed 30 min to cure.

A rapid method of monitoring (at least qualitatively) the tension of the PVC after being bonded to a panel was provided by a simple deflection-load apparatus devised and calibrated for each PVC thickness to be tested. Tension measurements were thus made immediately after the PVC bonds had been completed. Each panel was then brought to the model and filled (when required) with the chosen fluid through a small resealable port. A second port was used to exhaust all air within the panel cavity so that a complete and level quantity of fluid could be achieved. As a final assembly step, each panel was oriented with its longest dimension in the direction of flow and the neighboring rims of adjacent panels made smooth and continuous with 0.005 cm (0.002 in.) mending tape. It was possible to recheck the skin tension on each panel for models 2 and 3 at this time. Completed models showing typical test surfaces are presented in figures 9 through 11.

To limit the errors caused by thermal distortions within the mechanical loop formed by the model, support struts, and test section floor, the tunnel was first brought up to 22 m/s and maintained for 15 min. The tunnel was then cycled between 0 and 22 m/s to further exercise the flexures and transducers until the measured profile drag repeated to within required error bounds. Once the desired accuracy was attained, data were recorded at a maximum of three different velocities before returning for a zero reading. Each data point was actually the result of an average taken over one minute so that the effects of large-scale flow perturbations could be minimized. The sets of data points overlapped to allow a check of repeatability, and the entire collection of data sets was discarded if the desired error bound was exceeded. Once data were obtained over the full velocity range, a model calibration was immediately performed using dead weights. In the case of models 2 and 3, the final step was to repeat the tension measurements on each of the four panels.

## RESULTS

Profile drag measurements for each of the model configurations defined in table 1 are presented in figures 12 through 24. Data were obtained over a dynamic pressure range from 50 to 1000 pascals (Re = 1.6 to $7.4 \times 10^6$ based on a 2.65 m model chord). During the course of this experiment the tunnel air temperature ranged from 10° C to 21° C; however, the variation during any given run was normally less than 0.5° C.

Although thermal effects on skin tension were judged to be minimal during a given run, there still remained some concern that the PVC might relax due to plastic creep. To address this question, the skin tensions were examined before and after each run in the two cases where air served as the damping substrate; however, only nominal variations were found. Hence, in all cases where foam was not used (models 2 through 8), the skin tensions reported are those measured just after being bonded to the panels and prior to introducing any damping liquid. In those cases involving foam (models 9 through 11), the skin tension could not be directly measured and had to be inferred from the dead-weight arrangement used in preparing the PVC for model 8 (a nonfoam case).

The rigid-plate model was taken as the standard reference case against which all other configurations would be compared. Theoretical estimates indicate that the skin friction developed on this portion of the model was approximately 15 percent of the profile drag. It is believed that the error bounds maintained throughout the test were sufficiently small to expose any significant and practical benefits from the compliant surfaces studied.

The faired curve through the data points for the rigid reference case (fig. 12) also appears with the sets of discrete data given for each of the other model configurations. After examination of these results it is clear that in spite of the various parameters considered, none were successful in rendering a lower profile drag than had been obtained with the traditional rigid surface.

During numerous cases, traveling waves were observed to occur at the higher freestream velocities. The lower the skin tension, the greater the likelihood that waves would appear. Although no special effort was made to record their behavior in detail, some general characteristics were noted. Wave amplitudes appeared to reach 1 cm, while wave lengths were on the order of 30 cm to 60 cm. Wave speeds were quite dependent on the viscosity of the damping fluid. For example, speeds were

observed around 0.6 m/s with air substrates, 0.15 m/s with water, and 0.02 m/s with the polyethelene oxide solution.

## CONCLUSIONS

All configurations were found to yield profile drags equal to or slightly higher than that obtained for the conventional rigid surface case. Although the variety of compliant materials tested was limited, the results indicate that the potential for practical drag-reducing applications will be limited to either high-density or high-speed flows where more sensible pressure perturbations occur.

Ames Research Center, NASA
and
U. S. Army Air Mobility R&D Laboratory
Moffett Field, California, June 11, 1974

## REFERENCES

1. Looney, R. W.; and Blick, E. F.: Skin Friction Coefficients of Compliant Surfaces in Turbulent Flow. J. Spacecraft and Rockets, vol. 3, no. 10, Oct. 1966, pp. 1562–1564.

2. Blick, E. F.; and Walters, R. R.: Turbulent Boundary-Layer Characteristics of Compliant Surfaces. J. of Aircraft, vol. 5, no. 1, Jan.–Feb. 1968, pp. 11–16.

3. Blick, E. F.; Walters, R. R.; Smith, R.; and Chu, H.: Compliant Coating Skin Friction Experiments. AIAA Paper No. 69-165, Jan. 1969.

4. Lissaman, P. B. S.; and Harris, G. L.: Turbulent Skin Friction on Compliant Surfaces. AIAA J., vol. 7, Jan. 20–22, 1969, pp. 1625–1627.

5. Anon.: Standard Methods of Testing Slab Flexible Urethane Foam, American Society for Testing and Materials, Annual Book of ASTM Standards, pt. 28, D 1564, 1971.

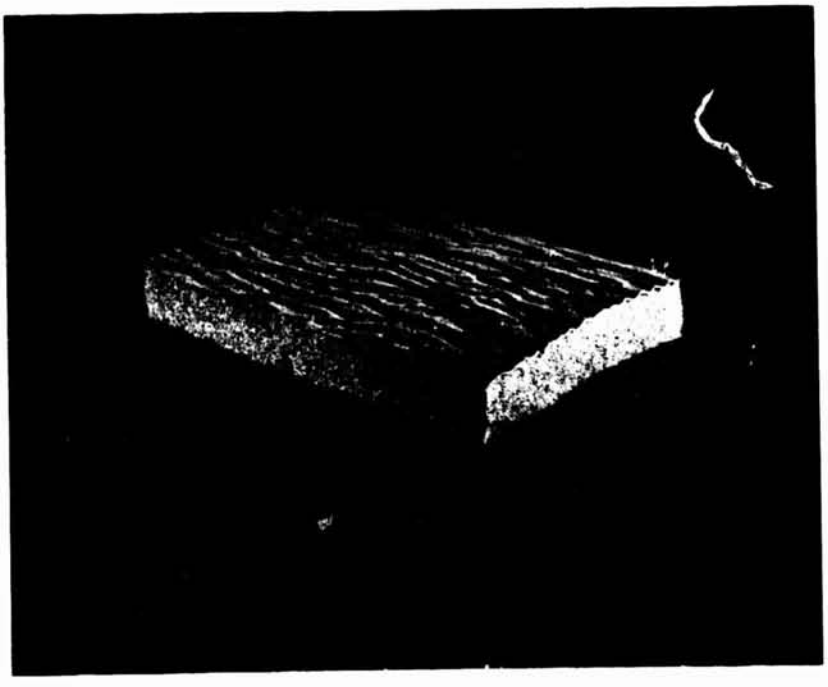

(a) Flexible 70 PPI polyurethane foam with integral skin.

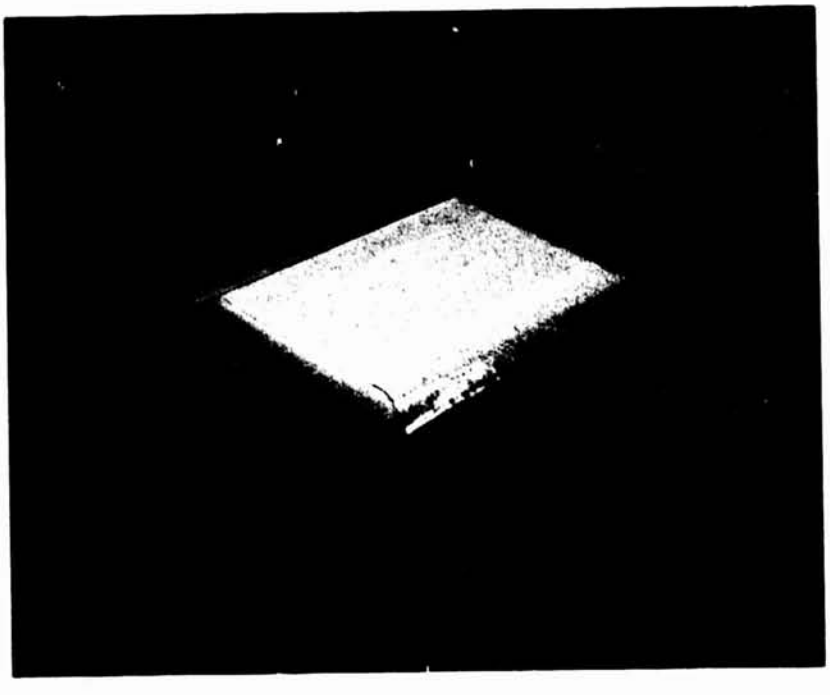

(b) Flexible 45 PPI polyurethane foam with polyvinylchloride skin.

Figure 1. Types of foam base compliant materials used.

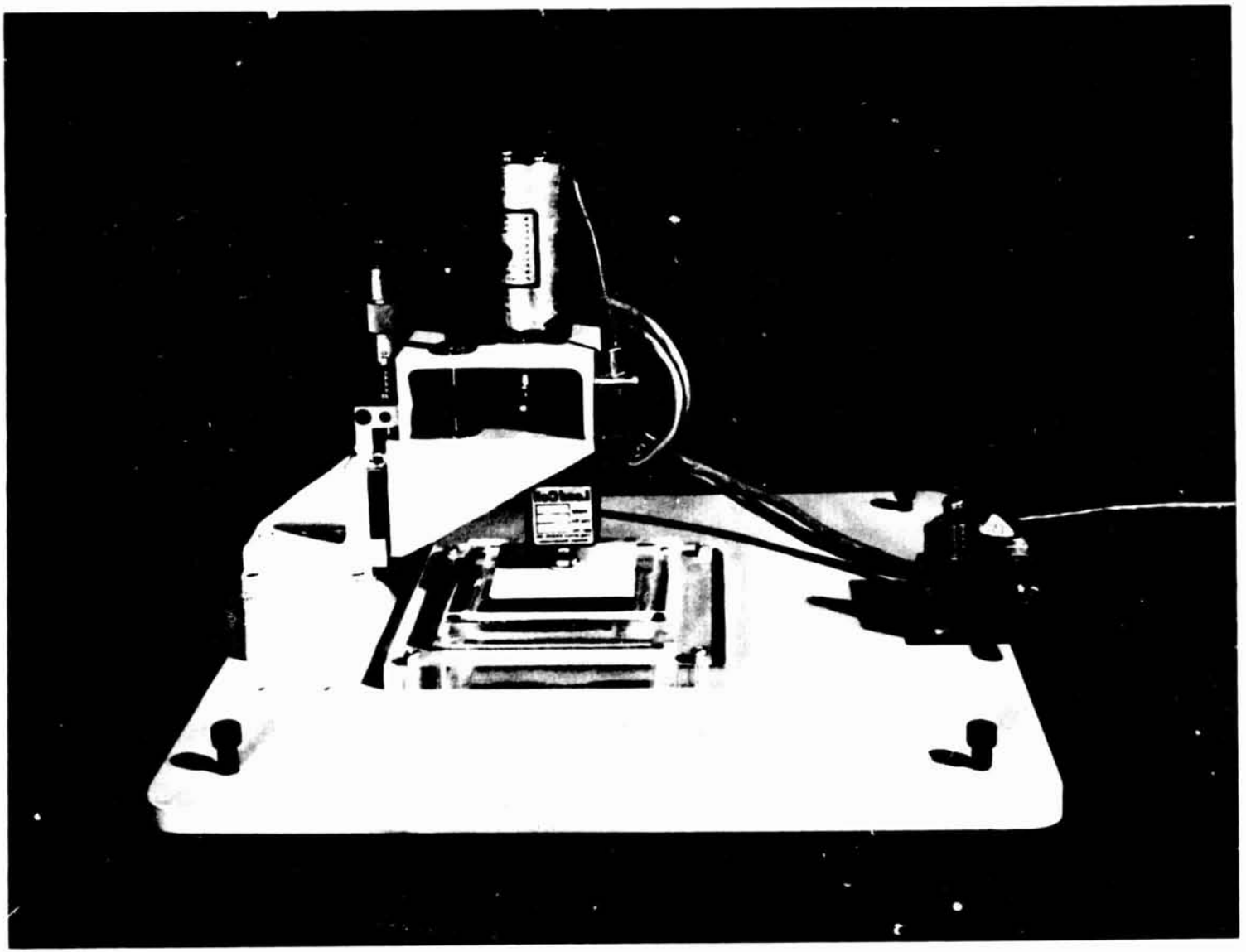

Figure 2. Compression load deflection apparatus.

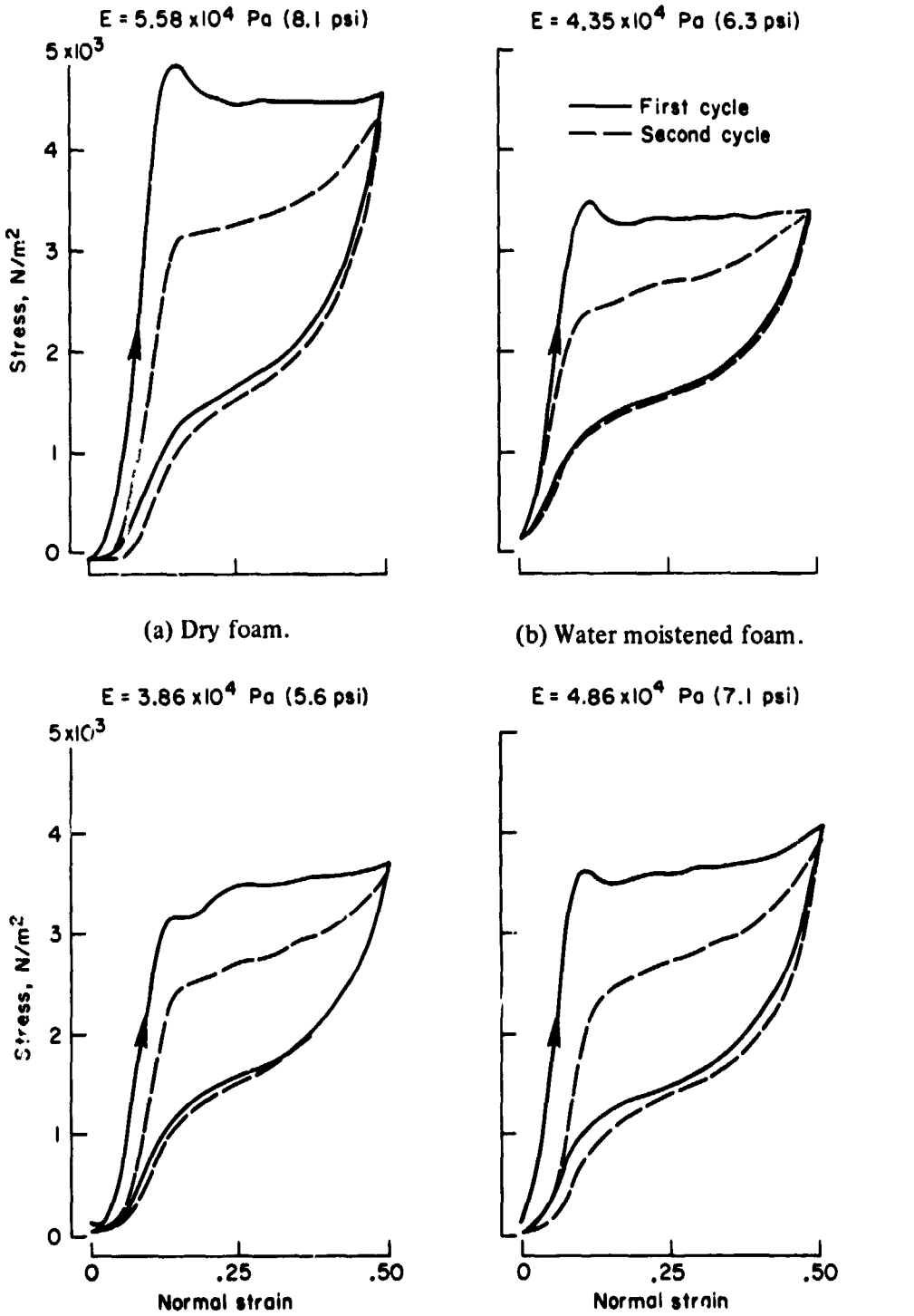


Figure 3.– Normal stress-strain behavior of 45 PPI foam subject to a ramp deformation at a compression and retraction rate of 2.5 cm/min.

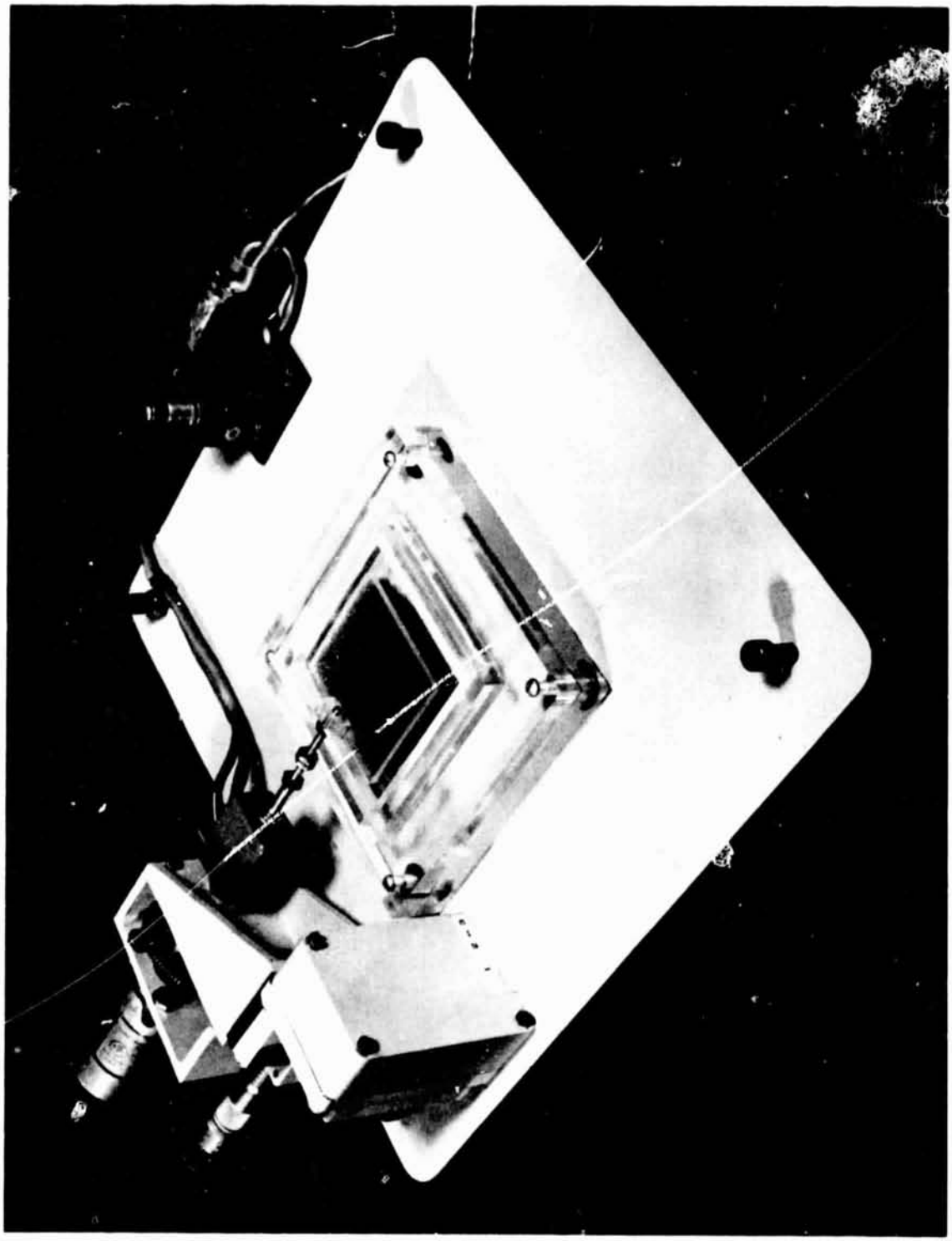

Figure 4.– Shear load deflection apparatus.

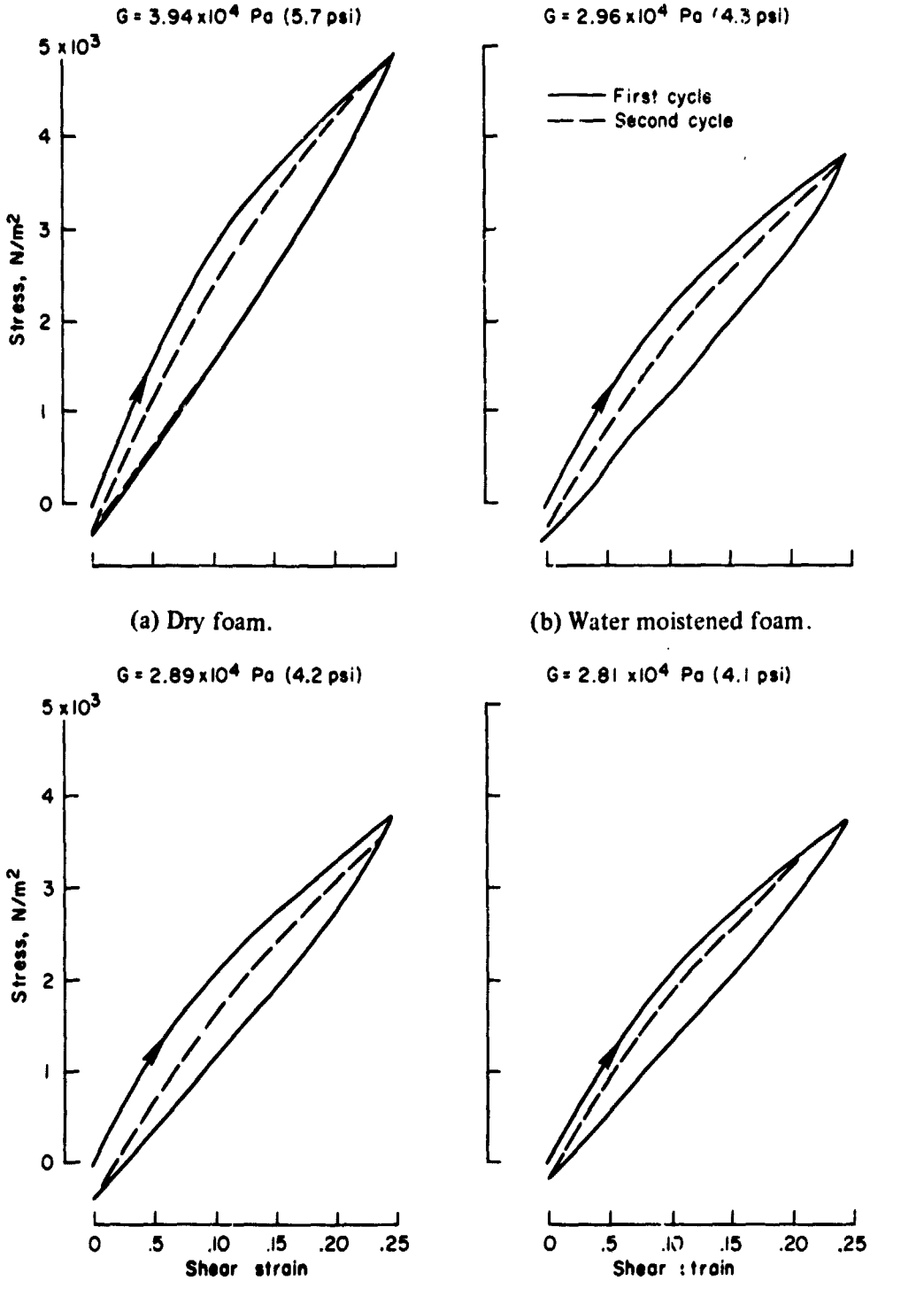


(a) Dry foam.

(b) Water moistened foam.

(c) Water flooded foam.

(d) Water/polyethelene oxide flooded foam.

Figure 5.– Shear stress-strain behavior of 45 PPI foam subject to a ramp deformation at a relative deflection and retraction rate of 2.5 cm/min.

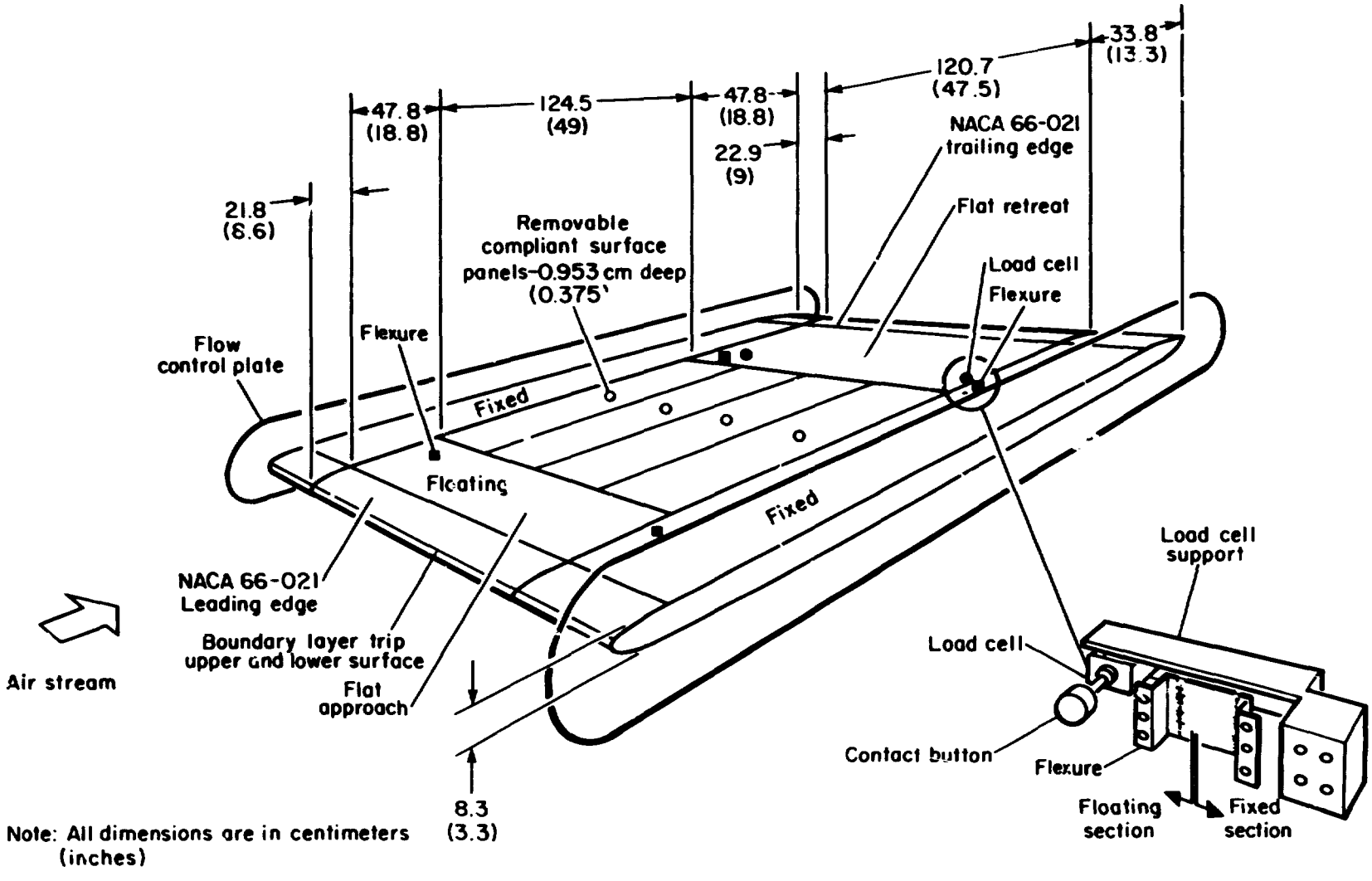


Figure 6.– Model components and dimensions.

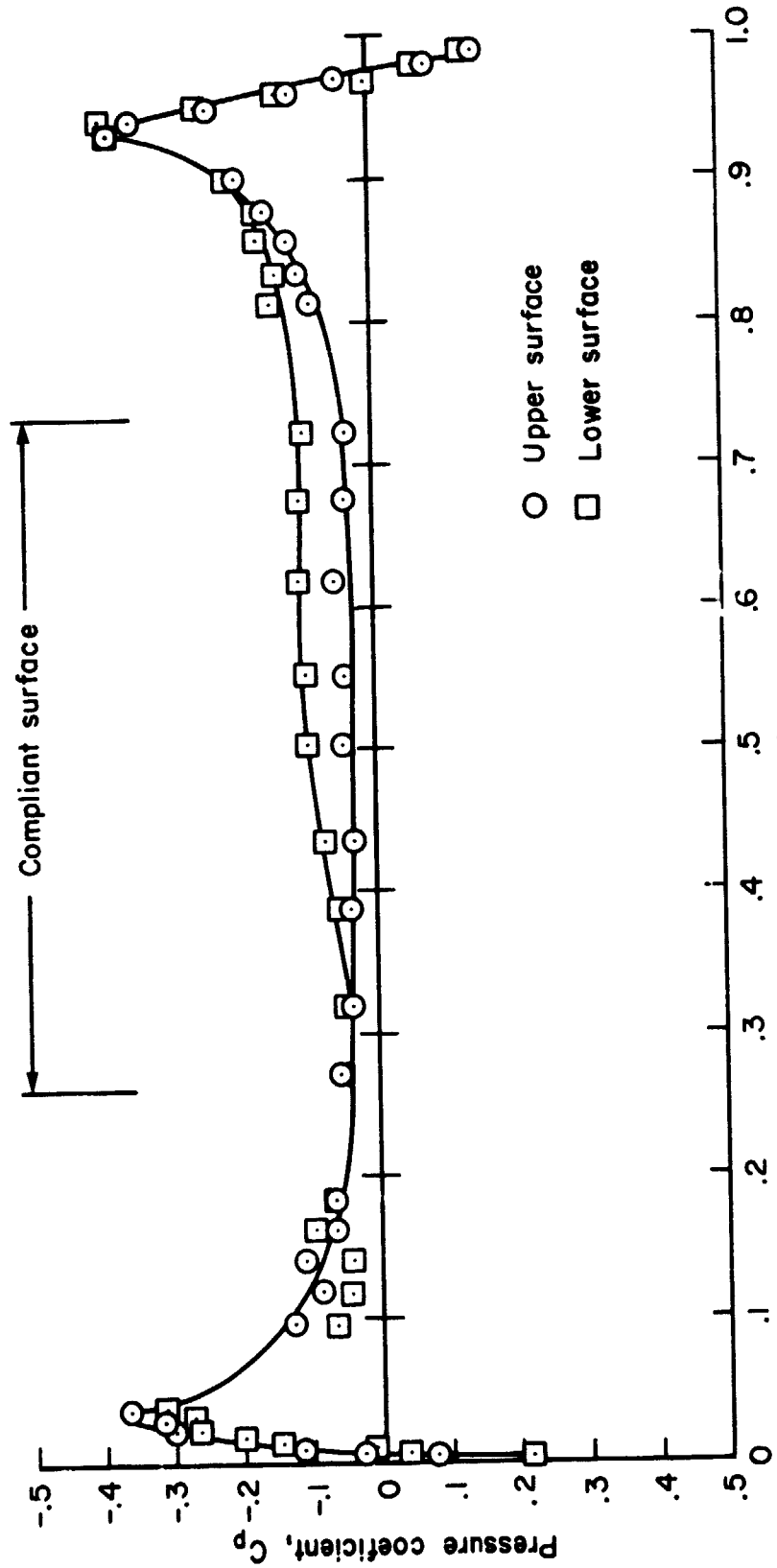


Figure 7.– Pressure distribution over model at $q$ = 1005 N/m$^2$ (21 psf).

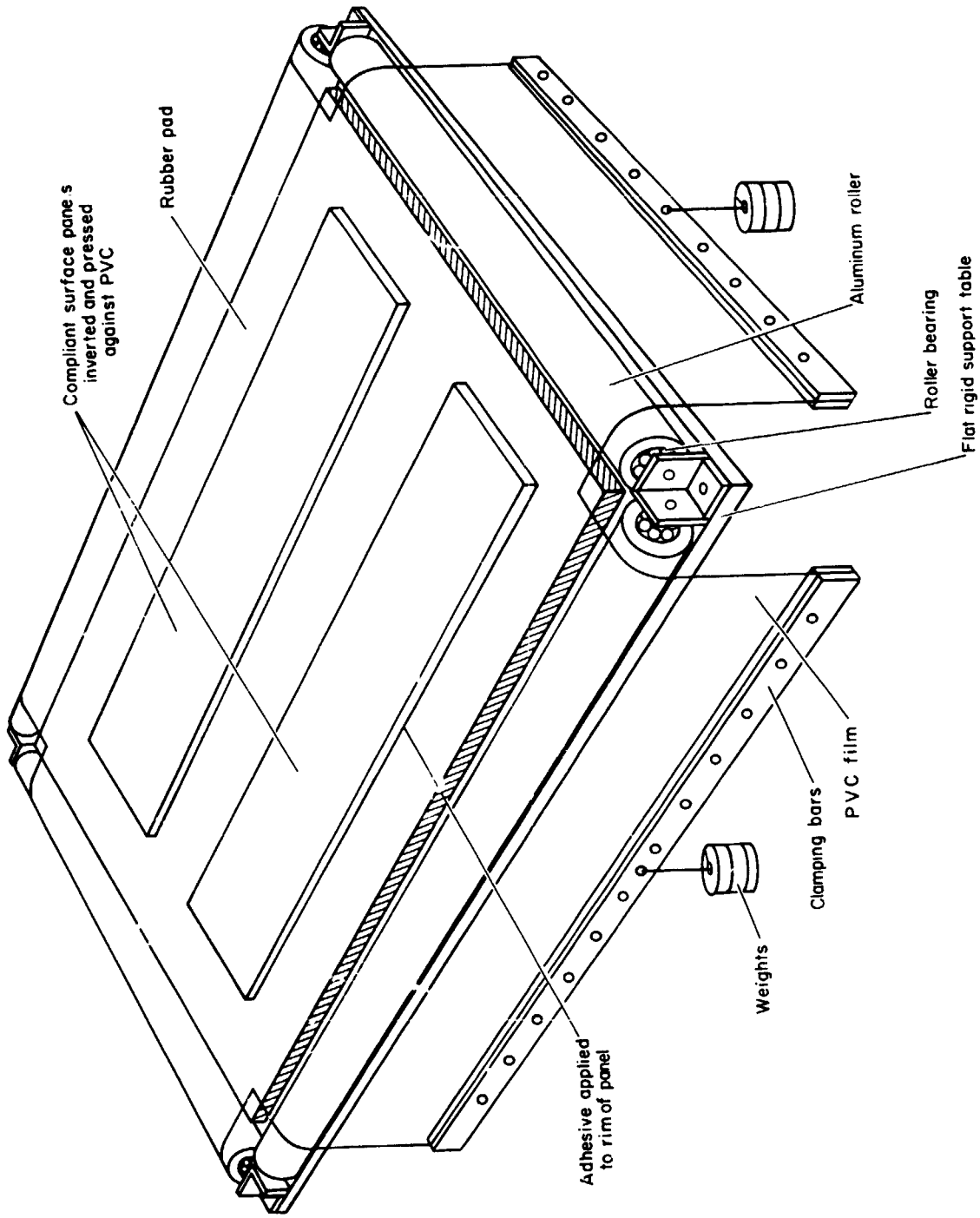


Figure 8.– Compliant panel preparation apparatus.

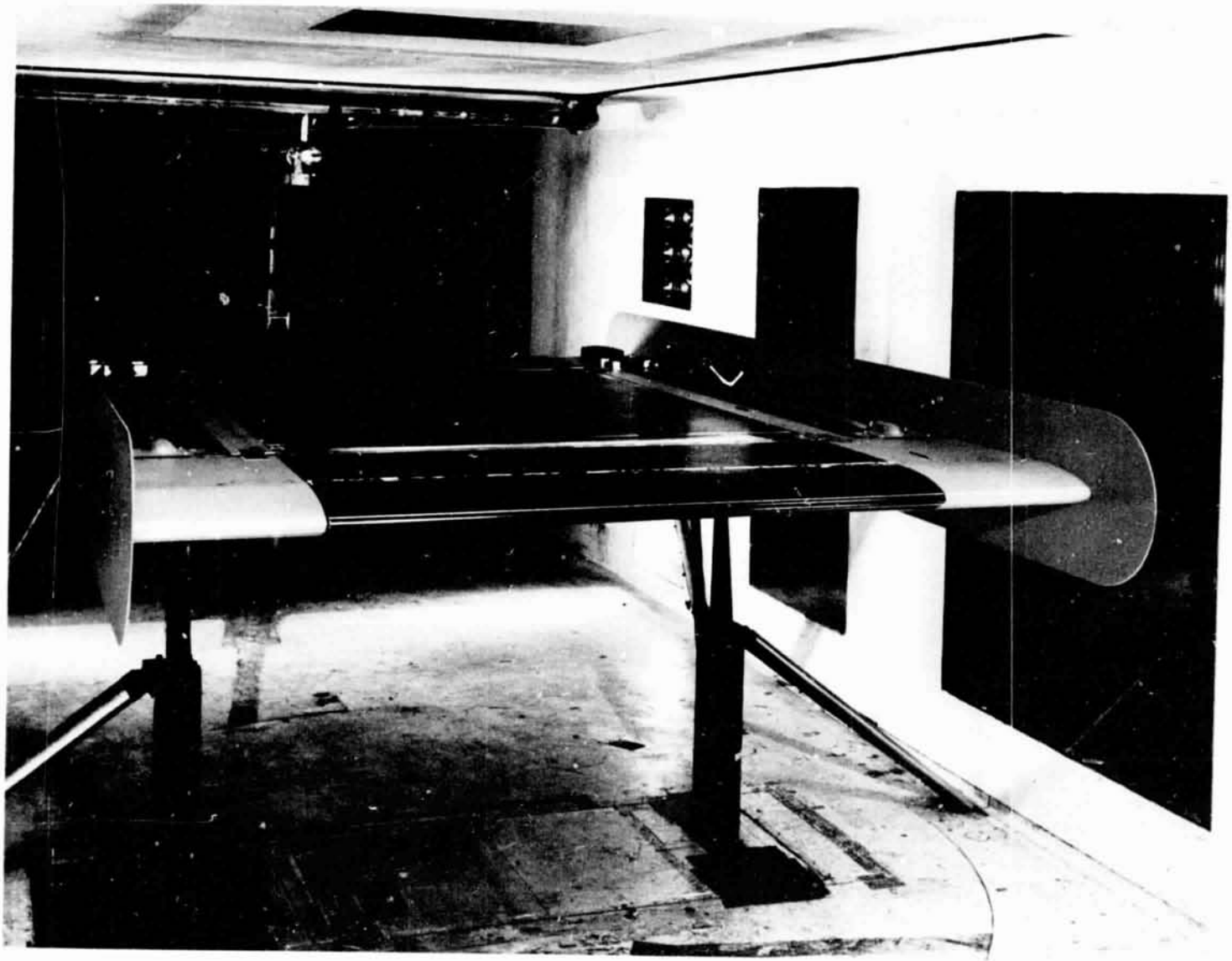

Figure 9.— Frontal view of model with rigid reference surface in place.

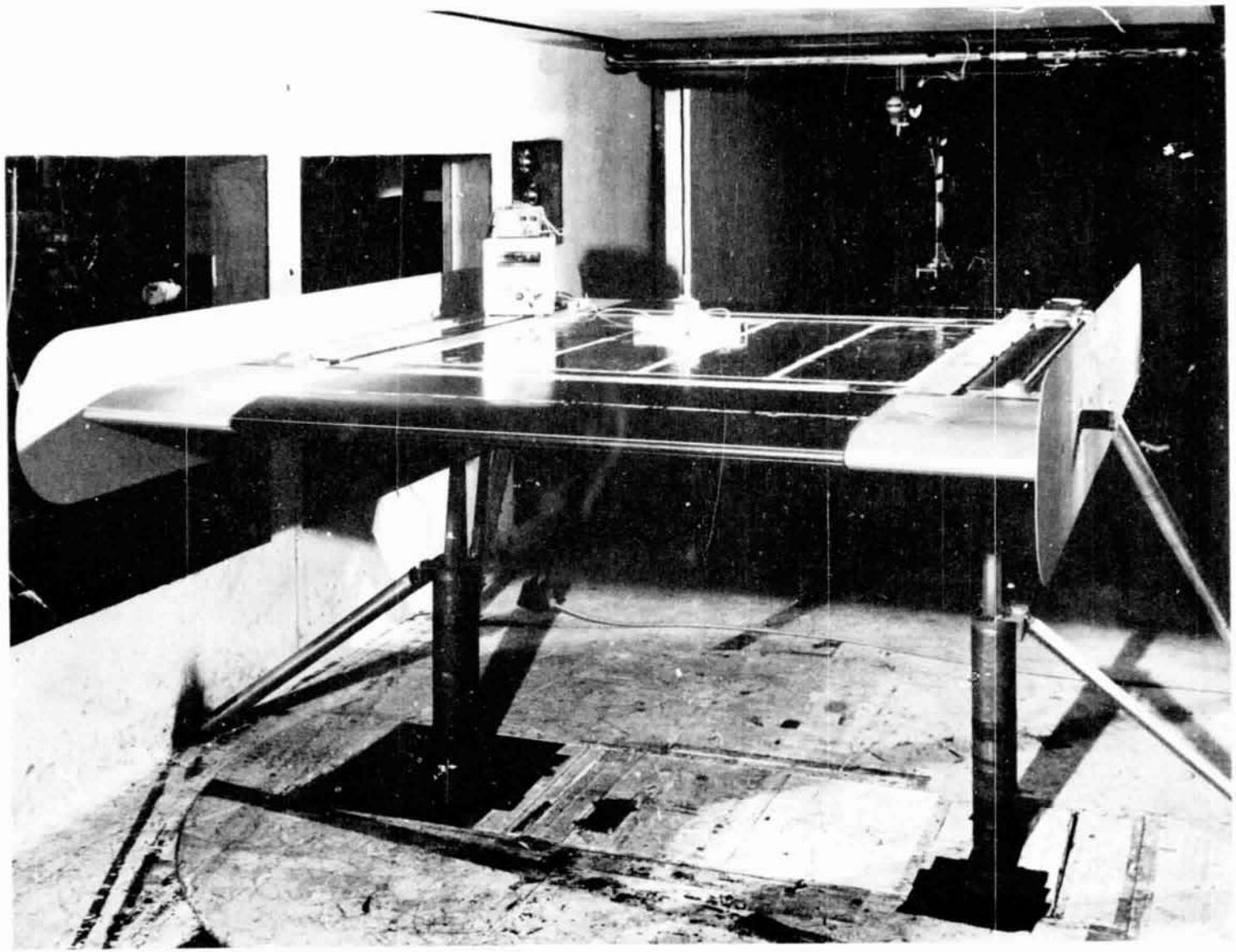

Figure 10.— Frontal view of model showing four compliant surface panels and the surface tension monitoring device.

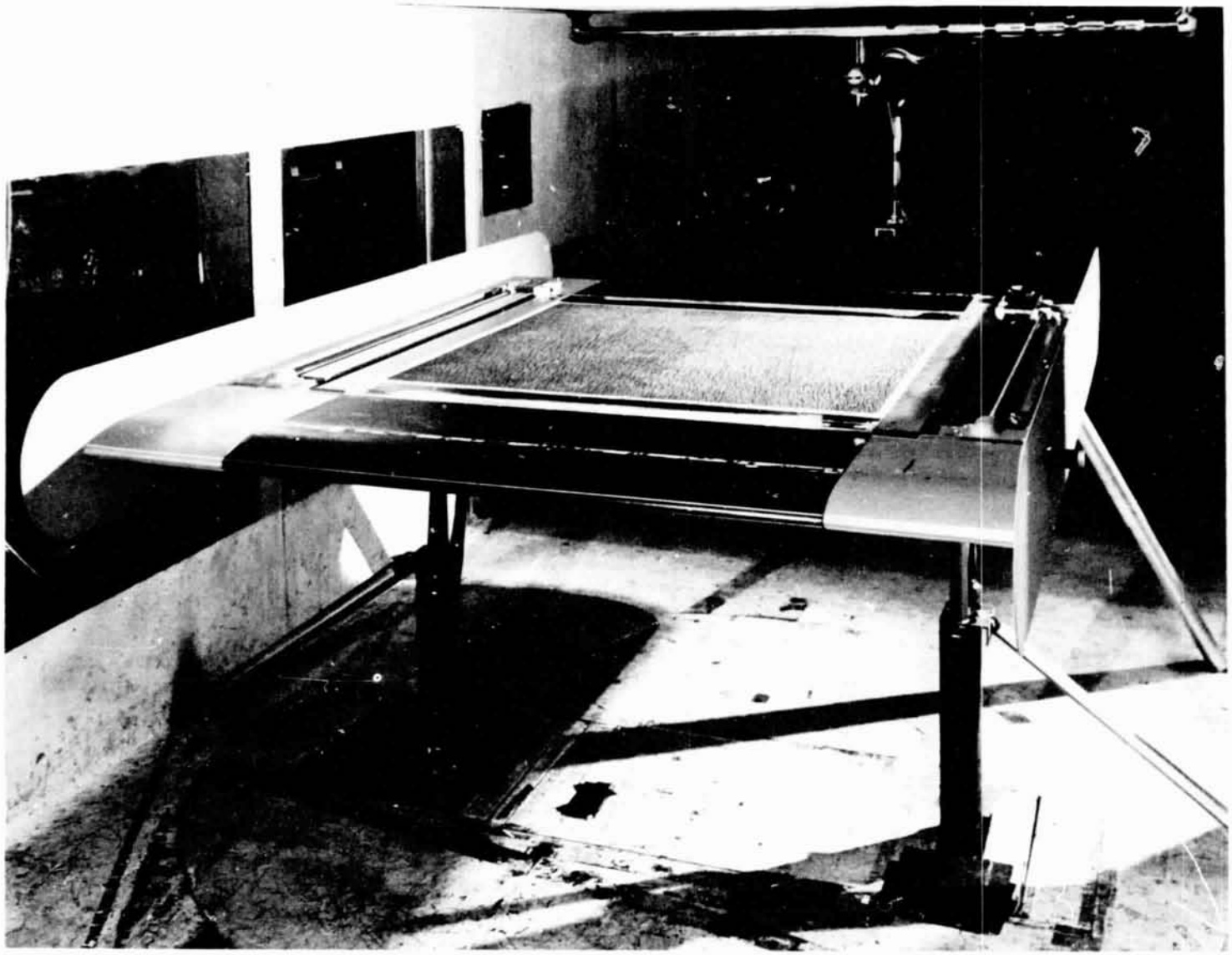

Figure 11.— Frontal view of mocel with texturized integral skin foam positioned with the grain parallel to the direction of flow.

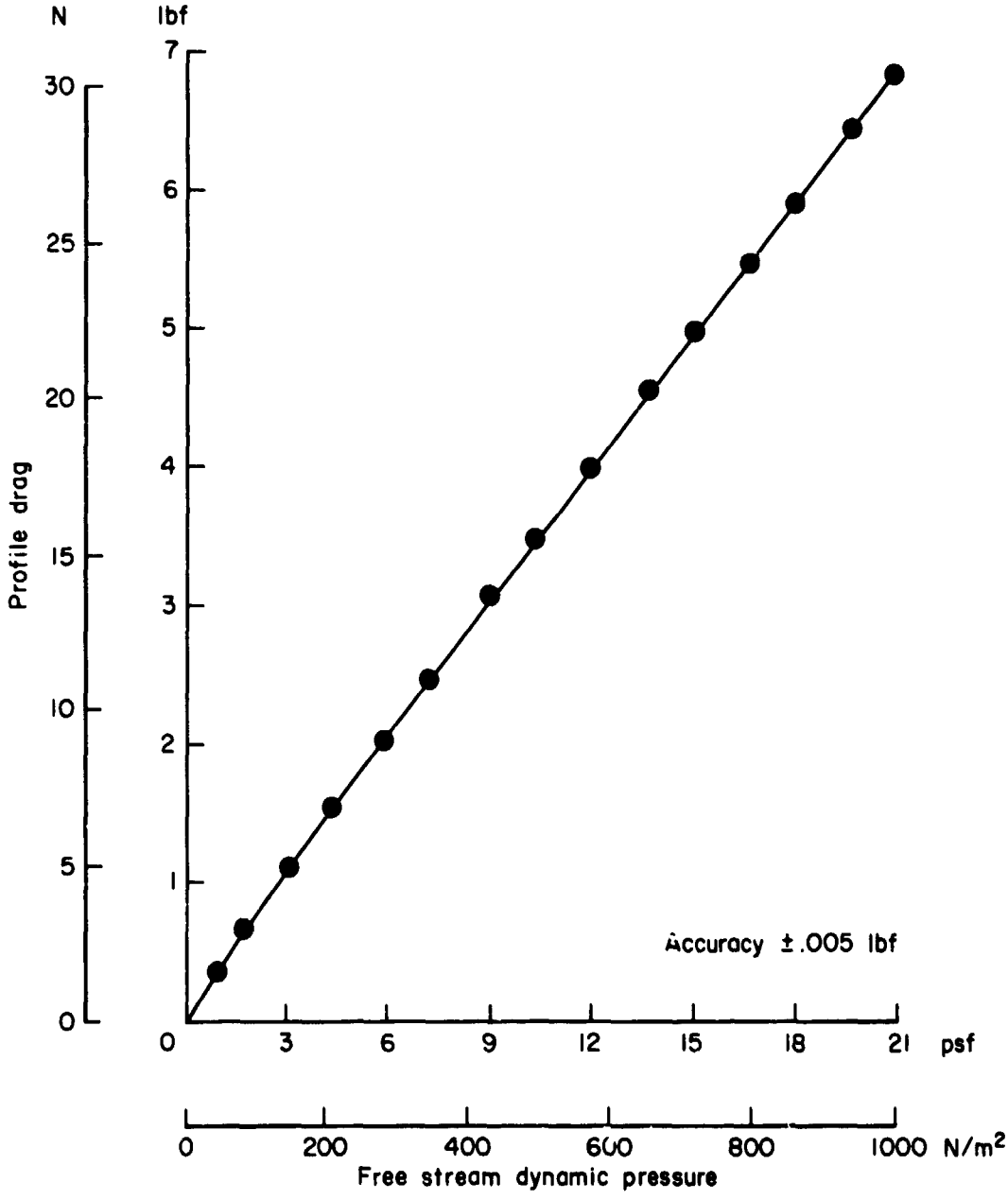


Figure 12.– Model 1 profile drag: rigid plate.

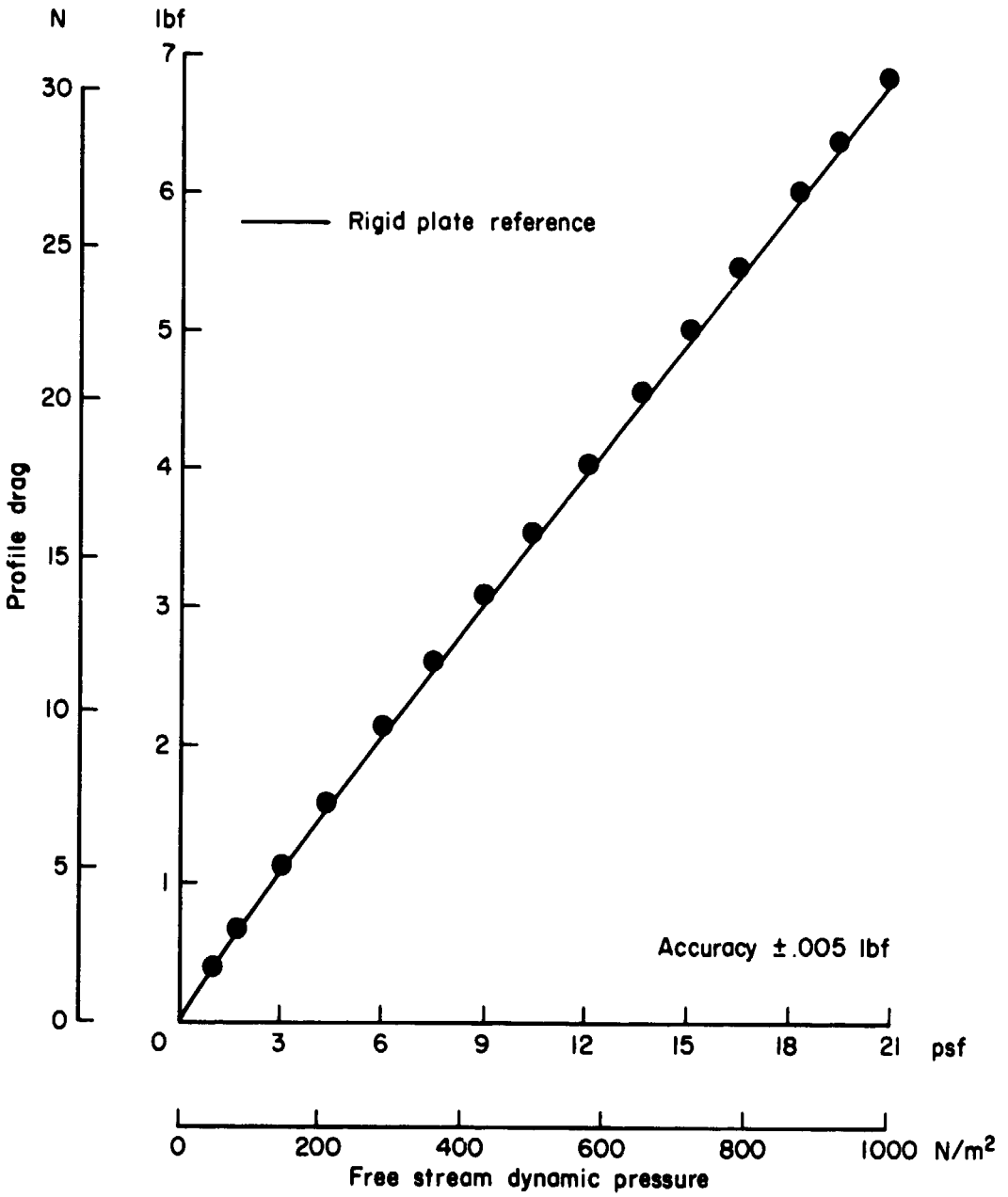


Figure 13.– Model 2 profile drag: 0.005 cm PVC stretched to 0.40 N/cm over air cavity. Traveling waves observed for $q > 718$ N/m$^2$.

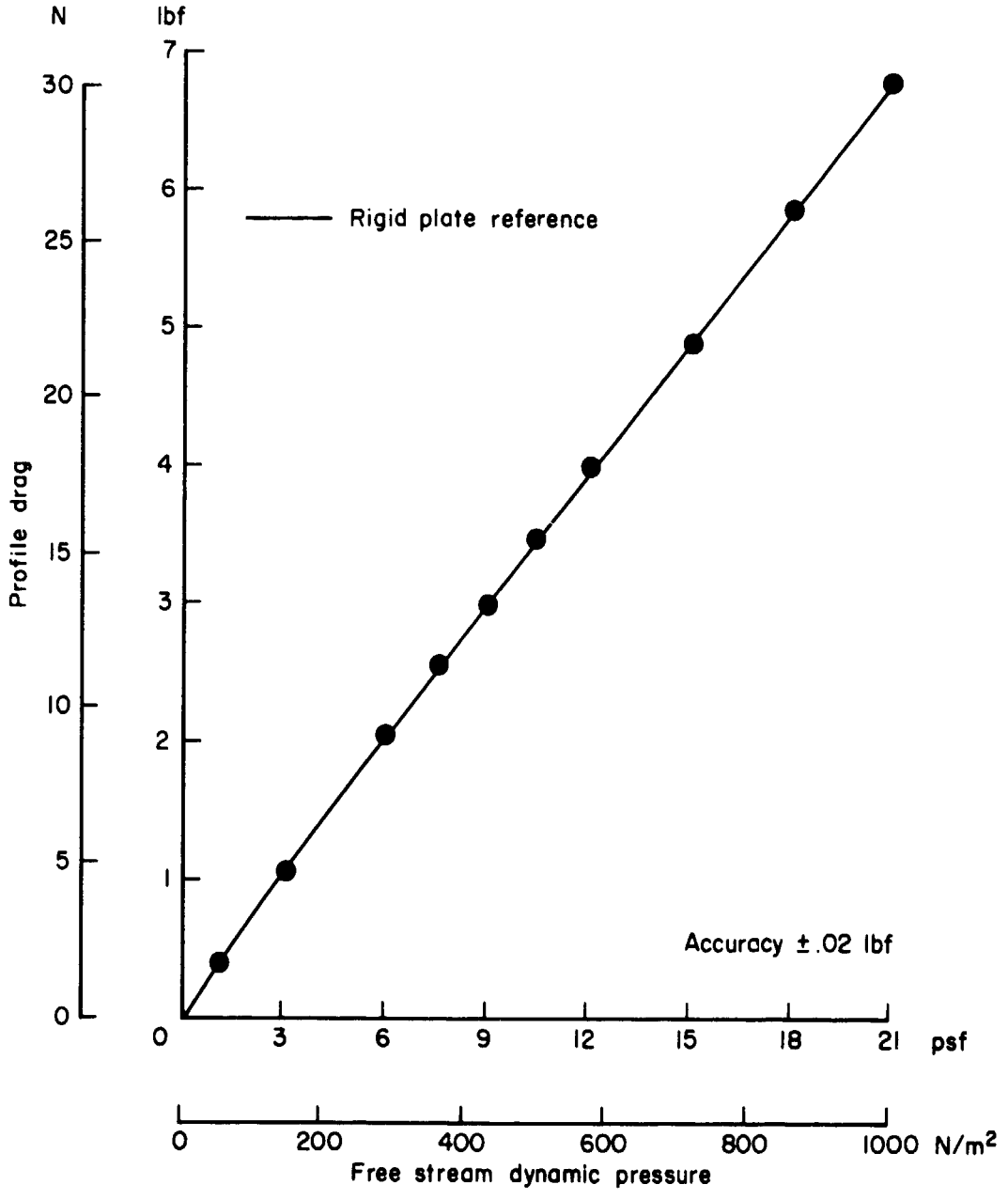


Figure 14.– Model 3 profile drag: 0.005 cm PVC stretched to 0.82 N/cm over air cavity. No traveling waves observed for $q < 1000$ N/m$^2$.

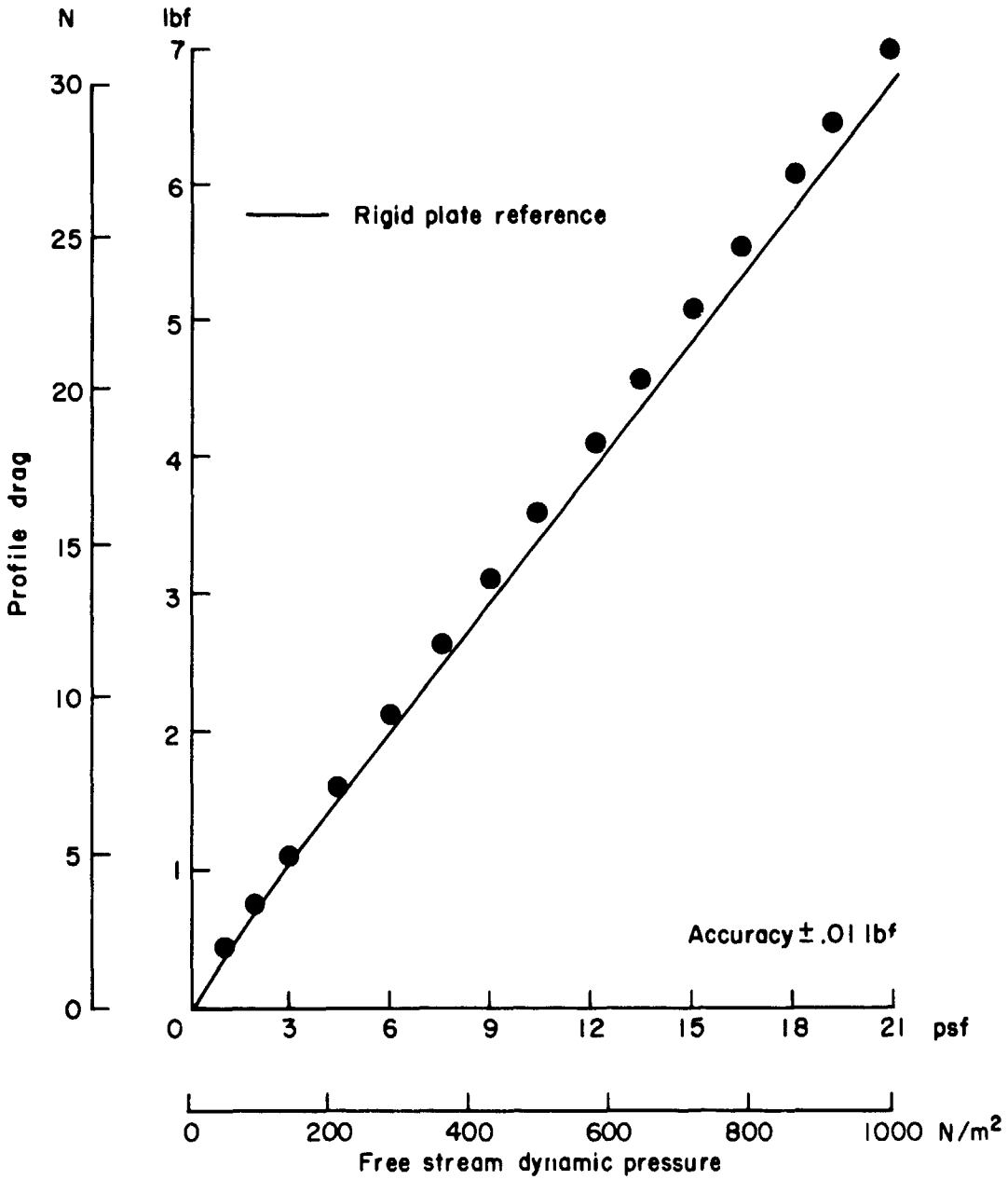


Figure 15.– Model 4 profile drag: 0.005 cm PVC stretched to 0.16 N/cm over water cavity. Traveling waves observed for $q > 575$ N/m$^2$.

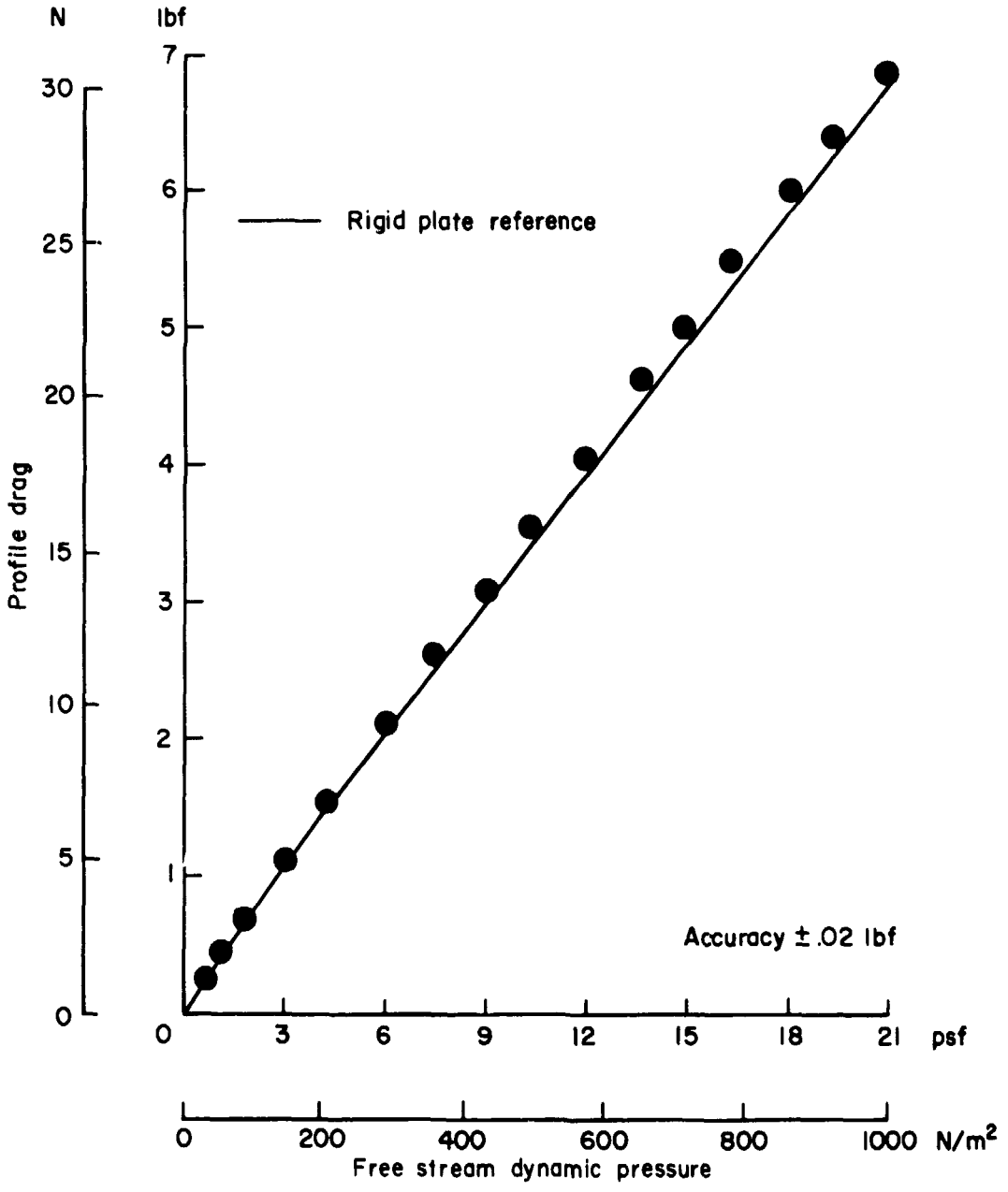


Figure 16.– Model 5 profile drag: 0.005 cm PVC stretched to 0.40 N/cm over water cavity. Traveling waves observed for $q > 766$ N/m$^2$.

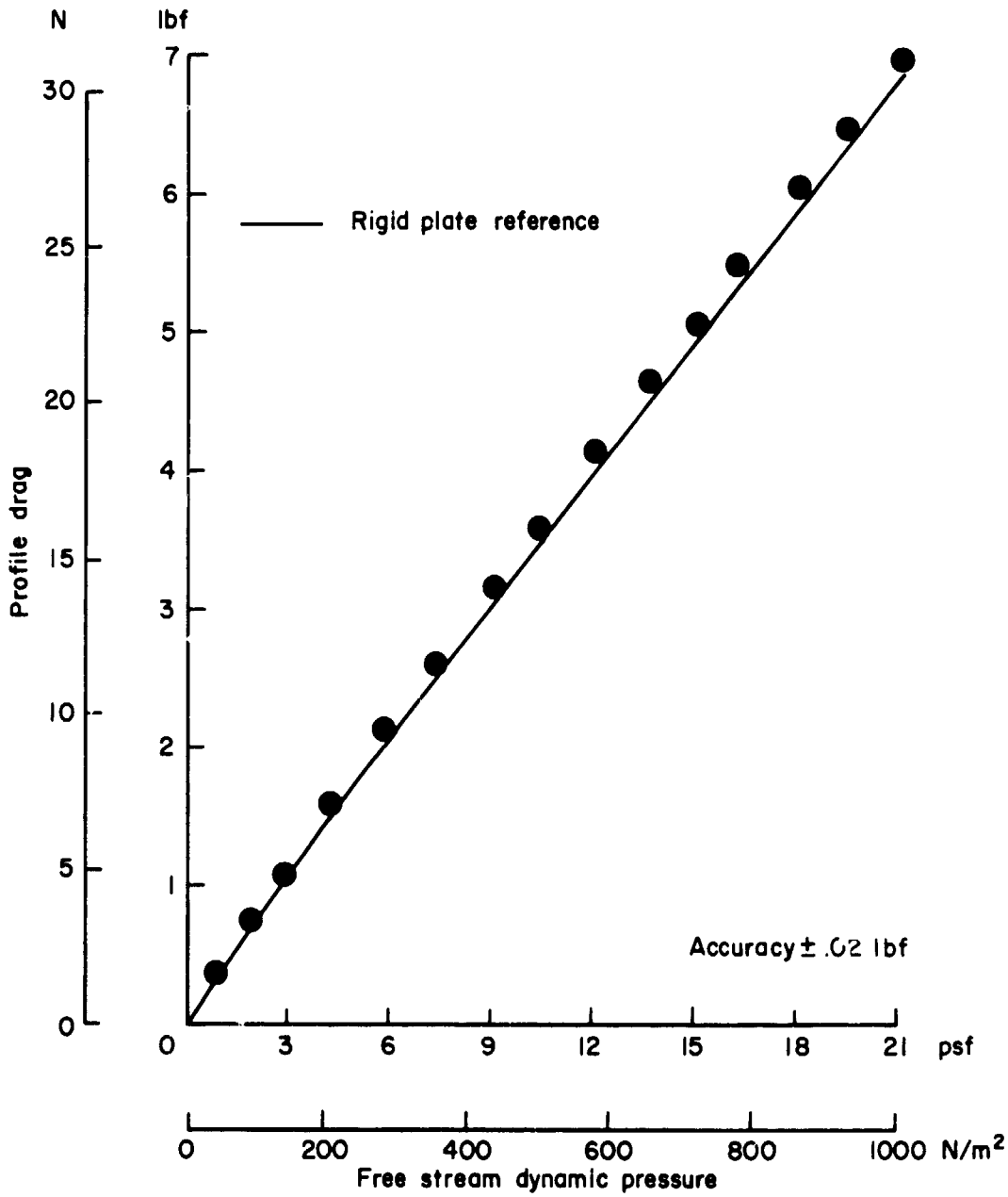


Figure 17.– Model 6 profile drag: 0.005 cm PVC stretched to 0.82 N/cm over water cavity. No traveling waves observed for $q < 1000$ N/m$^2$.

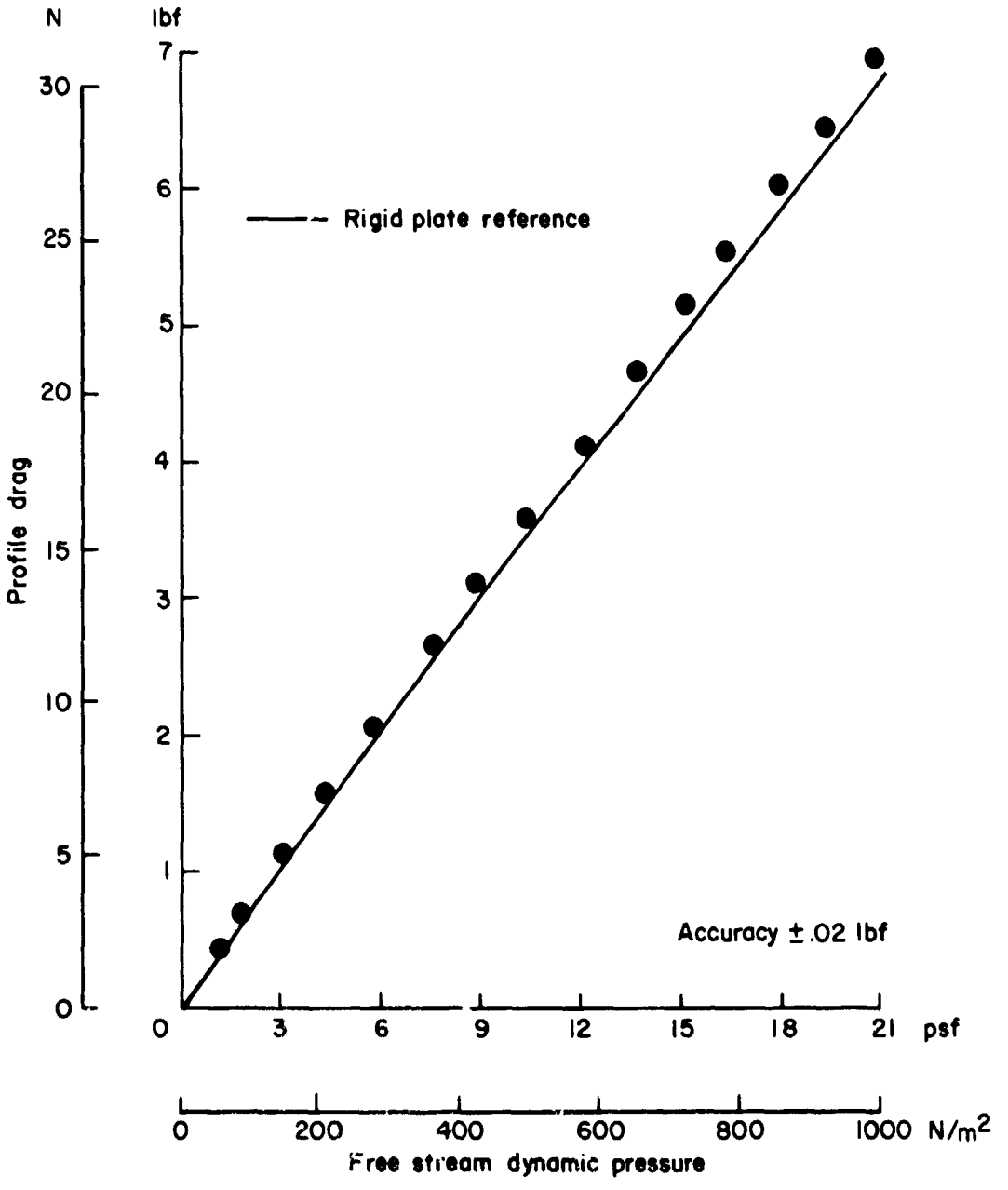


Figure 18.– Model 7 profile drag: 0.010 cm PVC stretched to 1.07 N/cm over water cavity. Traveling waves first appear at $q = 1000$ N/m$^2$.

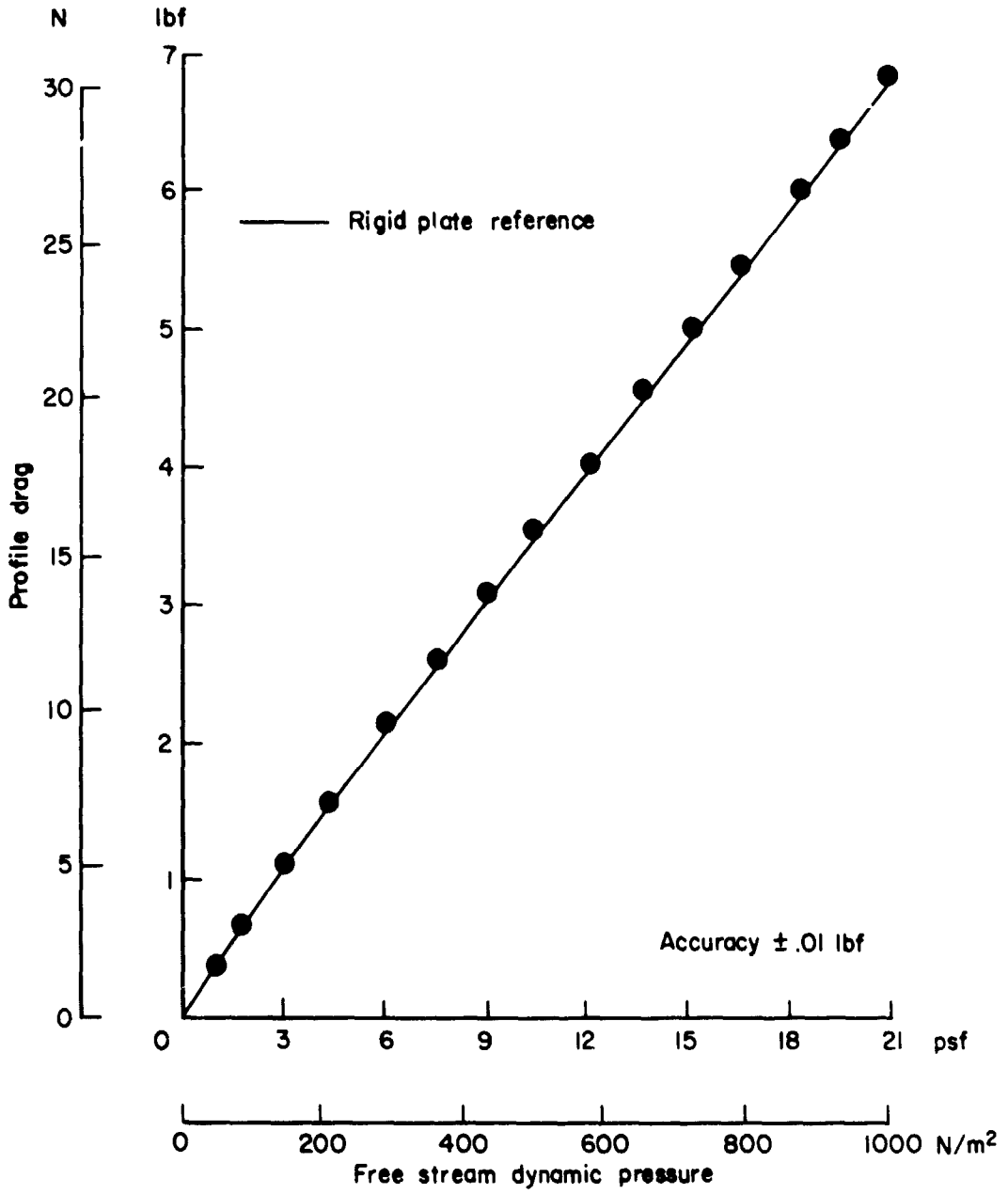


Figure 19. Model 8 profile drag: 0.005 cm PVC stretched to 0.26 N/cm over water/polyethelene oxide cavity. Traveling waves observed for $q > 862$ N/m$^2$.

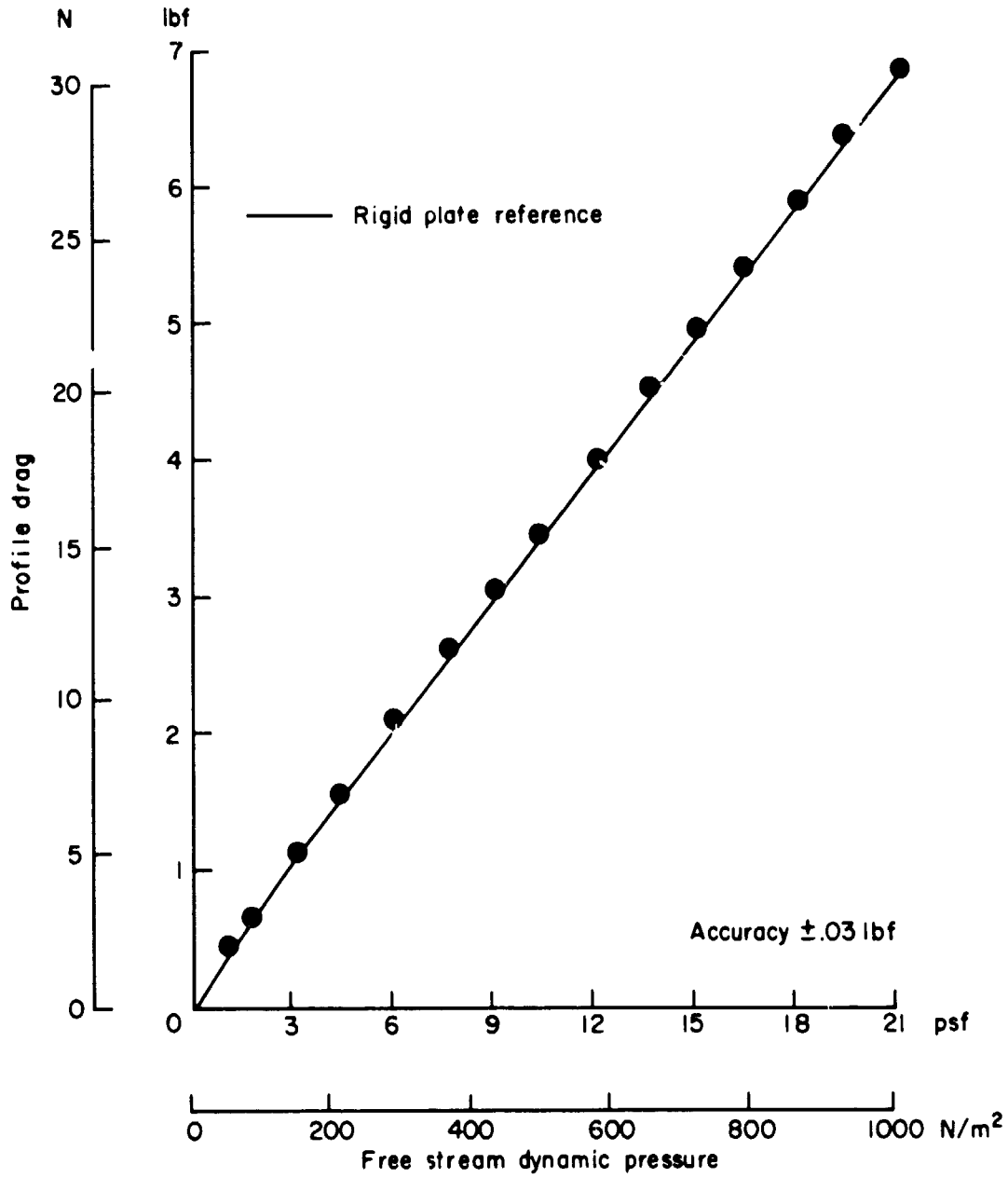


Figure 20. Model 9 profile drag: 0.005 cm PVC stretched to 0.26 N/cm over dry foam. No traveling waves observed for $q < 1000$ N/m$^2$.

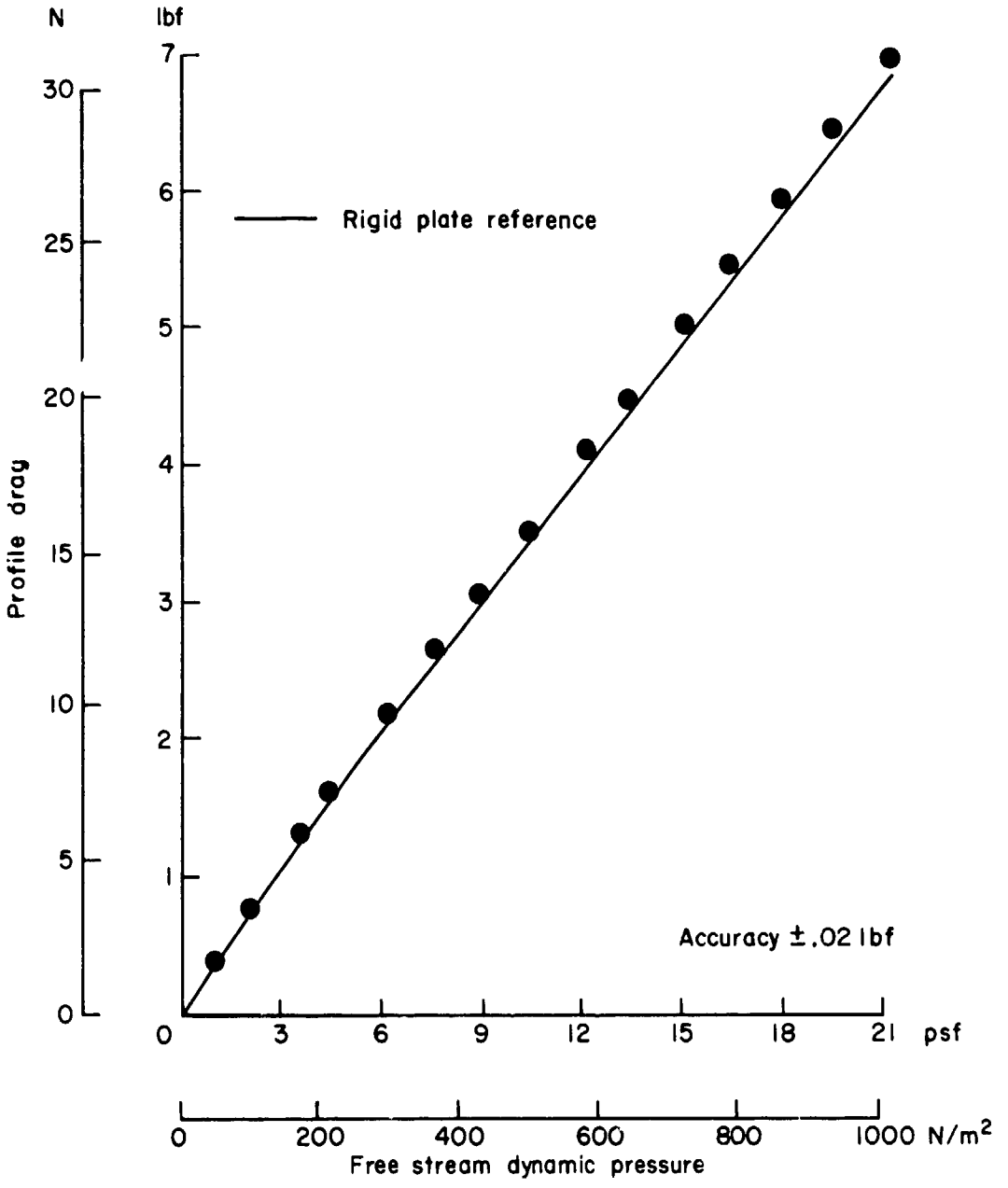


Figure 21.– Model 10 profile drag: 0.005 cm PVC stretched to 0.26 N/cm over water flooded foam. No traveling waves observed for $q < 1000$ N/m$^2$.

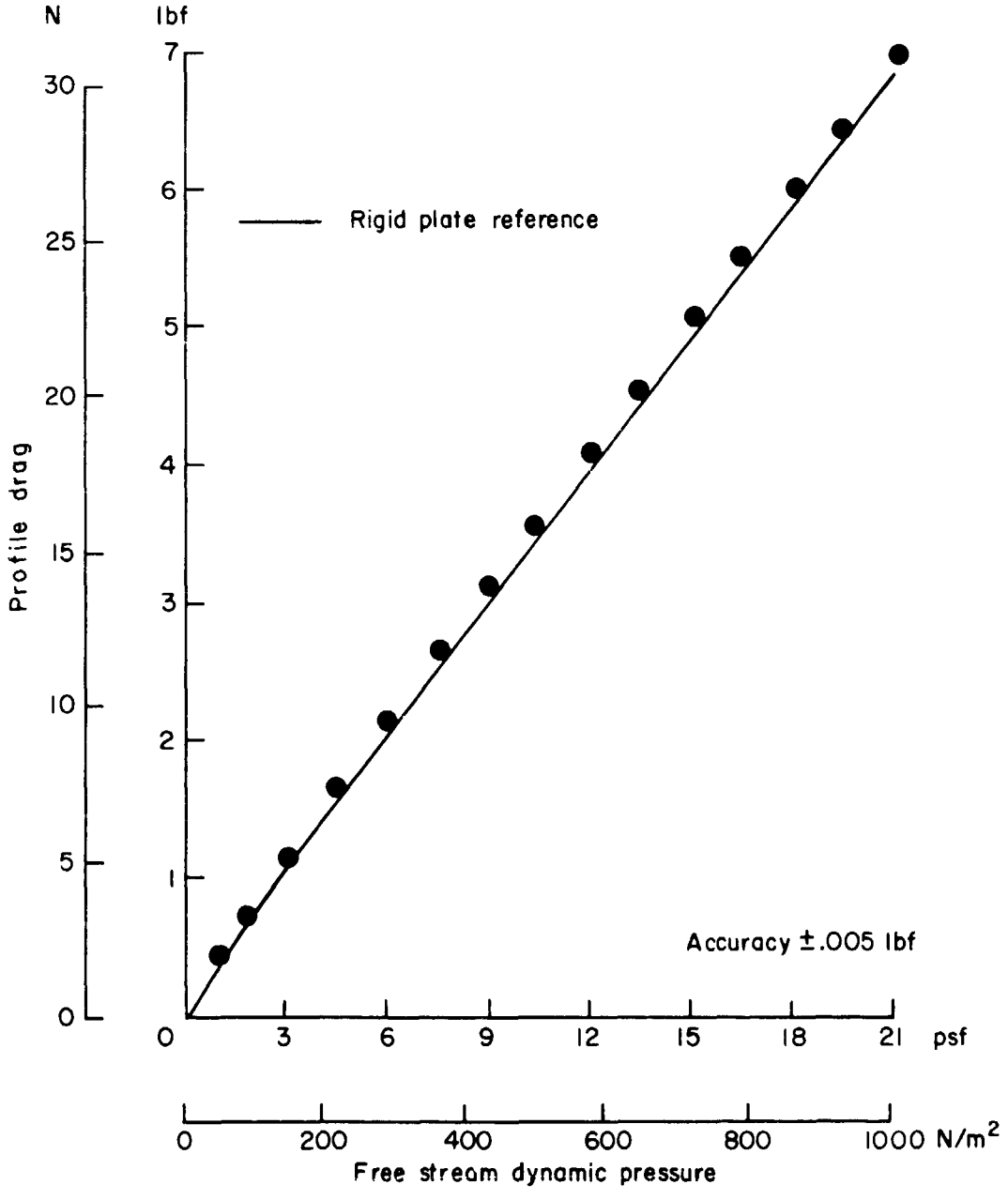


Figure 22.-- Model 11 profile drag: 0.005 cm PVC stretched to 0.26 N/cm over water/polyethelene oxide flooded foam. No traveling waves observed for $q < 1000$ N/m$^2$.

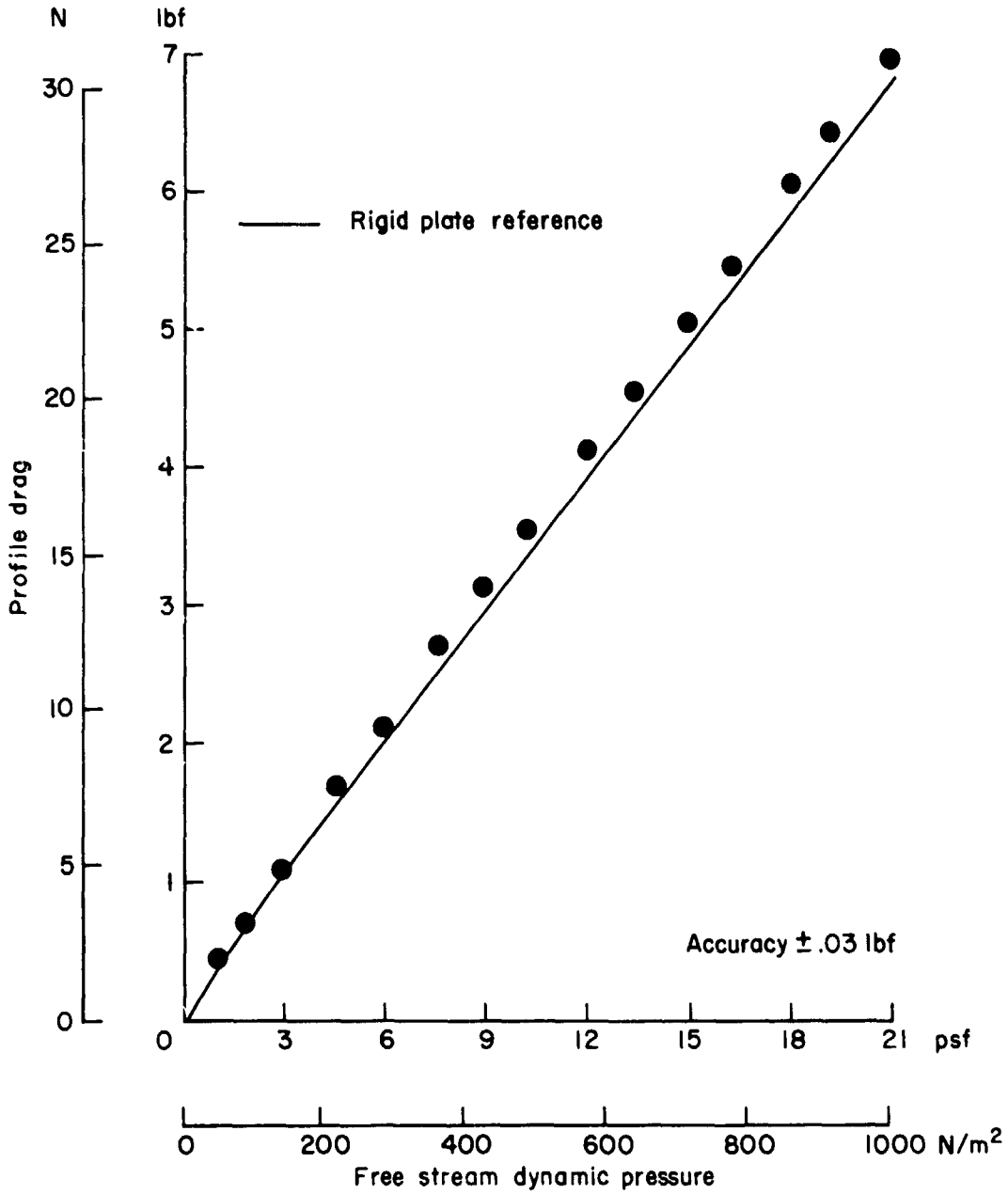


Figure 23.– Model 12 profile drag: integral skin foam with grain running parallel to flow direction. No traveling waves observed for $q < 1000$ N/m$^2$.

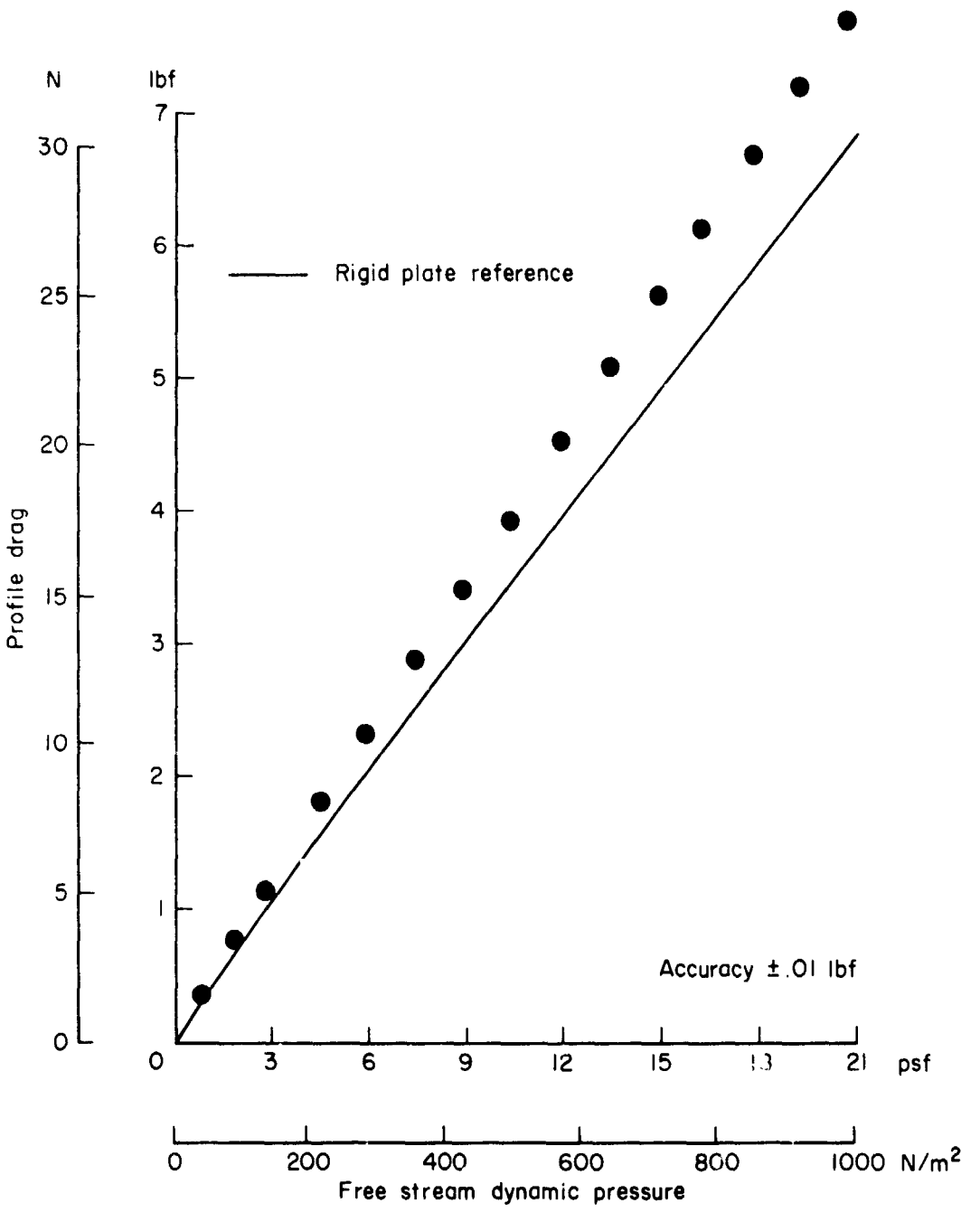


Figure 24. Model 13 profile drag: integral skin foam with grain running perpendicular to flow direction. No traveling waves observed for $q < 1000$ N/m$^2$.